INTERNATIONAL JOURNAL OF PHARMACOGNOSY AND CHEMISTRY
Content available at www.saap.org.in Online ISSN: 2582-7723

Open Access Review Article

CHEMOMETRIC STRATEGIES FOR SIMULTANEOUS QUANTIFICATION OF CO-EXISTING POLLUTANTS IN COMPETITIVE AND MULTICOMPONENT ADSORPTION SYSTEMS: A CRITICAL REVIEW

MAHA SALAH NASR

College of Food Science, AL-Qasim Green University, Babylon, Iraq.

DOI: https://doi.org/10.46796/ijpc.v7i2.949

ARTICLE HISTORY

Received on: 28-05-2026
Revised on: 14-06-2026
Accepted on: 26-08-2026

***Keywords*:** Competitive adsorption; Multicomponent systems; Chemometrics; Derivative spectrophotometry; Partial least squares; Multivariate curve resolution; Analytical figures of merit.

***CORRESPONDING AUTHOR**
Maha Salah Nasr

ABSTRACT

Adsorption studies are still, in the great majority of cases, reported for a single adsorbate, yet the effluents they claim to treat almost never contain one pollutant. Moving from one solute to two or three changes the experiment in a way that is easy to underestimate, because the analytical step itself becomes the limiting factor: the absorbance recorded at one wavelength can no longer be assigned to one species. This review examines how chemometric tools have been used, and occasionally misused, to recover individual concentrations of co-existing pollutants during competitive adsorption. We first set out the artefacts peculiar to adsorption supernatants: spectral overlap, adsorbent-derived colour, residual turbidity and pH-driven speciation. We then follow the methodological ladder from univariate remedies such as derivative and ratio-spectra techniques and the H-point standard addition method, through first-order multivariate calibration by principal component regression and partial least squares with wavelength selection and net analyte signal theory, up to second-order and multiway approaches such as curve resolution and parallel factor analysis, which retain accuracy in the presence of uncalibrated interferents. Neural networks and machine-learning regressors are discussed separately, since they address a genuinely nonlinear problem but carry their own validation burden. Throughout we insist on a point that most application papers pass over: competition factors, extended Langmuir constants and ideal adsorbed solution predictions inherit the uncertainty of the quantification step, so an unvalidated calibration propagates quietly into the thermodynamic conclusions. A minimum reporting set is proposed to make multicomponent removal data comparable between laboratories.

1. INTRODUCTION

Removal of dyes, pharmaceuticals, phenols and heavy-metal ions by adsorption is one of the most heavily published areas in applied environmental chemistry. What has not grown at the same pace is the realism of the systems studied. Real effluents are mixtures, and when two or more adsorbates share a finite set of surface sites the uptake of each is no longer what the single-solute isotherm predicts [1]. Competition may be antagonistic, synergistic or essentially non-interactive, and the classification depends on the adsorbate pair, the surface chemistry and the ionic composition of the solution [2]. Reviews of multicomponent isotherm modelling have compiled dozens of equations for such behaviour [3], and the dye literature has repeatedly identified multicomponent effluents as the case of practical interest [4].

The difficulty is that all of this modelling rests on one deceptively simple quantity: the residual concentration of each pollutant after contact with the adsorbent. In a single-solute experiment that quantity comes from a calibration line at the absorption maximum, and the procedure is so routine that it is usually described in one sentence. In a binary or ternary system, the same measurement is no longer defined, because the absorbance at any wavelength is a sum of contributions. Sev-

eral groups discovered this the hard way; Gao and co-workers abandoned direct spectrophotometric measurement for partial least squares after finding it inadequate for an overlapped anionic dye pair [5], and Hajati and colleagues reported that first-derivative treatment, which had worked elsewhere, simply failed for brilliant green and methylene blue [6].

Chemometrics offers a family of answers, from a second-derivative transform that costs nothing to multiway methods requiring a change of instrument. The literature applying them to adsorption is substantial but scattered, and rarely critical about its own assumptions. This review brings it together, sets out what each class of method actually guarantees, and shows how the choice of quantification strategy propagates into the competitive adsorption parameters that are the real object of the study.

2. THE ANALYTICAL BOTTLENECK IN MULTICOMPONENT ADSORPTION

2.1 Spectral overlap and the additivity assumption

Molecular absorption bands in the ultraviolet and visible regions are broad. Two cationic dyes of similar chromophoric class may have maxima separated by 30–60 nm, which sounds comfortable until one recognises that each band is 80–120 nm wide at half height. The consequence is that neither analyte has a wavelength at which it absorbs alone, as Figure 1 illustrates for a simulated pair. Any attempt to use the maximum of dye A therefore over-estimates A by the amount that dye B contributes there, and the bias grows as the experiment proceeds, because adsorption changes the two concentrations at different rates. Turabik's early binary study on bentonite made this explicit by comparing single- and binary-component uptake for basic red 46 and basic yellow 28, and the competition penalty she reported would have been unobtainable from raw absorbance [7].

All of the univariate remedies discussed below, and the classical multivariate ones as well, assume that the mixture spectrum is the linear sum of the pure-component spectra weighted by concentration. This assumption is usually reasonable at low concentration, but it is not automatic. Cationic dyes aggregate; several change protonation state within the pH range used in adsorption work; and ion pairing between an anionic and a cationic dye in the same beaker can produce a species whose spectrum belongs to neither parent. Additivity should be verified, not assumed, and a simple test, in which the spectrum of a physical mixture is compared with the sum of the individual spectra at the same nominal concentrations, takes half an hour and is almost never reported.

2.2 Artefacts that belong to the adsorption experiment itself

Beyond overlap, multicomponent adsorption supernatants carry interferences that pure-standard calibration does not see. Fine adsorbent particles that pass the filter contribute scattering across the whole spectrum; the effect is wavelength-dependent and mimics a baseline shift. Biosorbents are worse, since they leach coloured organic matter, and Besegatto and co-workers had to build a multivariate model explicitly to separate the colour contributed by one gram of mandarin peel from that of four dyes [8]. Engineered nanoparticles suspended in the sample cause the same problem in the ultraviolet, and a documented case with nano-Fe(OH)3 interfering in the determination of p-nitrophenol required acidification and masking before accurate results could be recovered [9]. Trace co-absorbing impurities are also more damaging than intuition suggests, because molar absorptivities differ by orders of magnitude, so a chemically negligible impurity can dominate the signal [10]. Finally, the competitive isotherm models themselves have been criticised on grounds that touch the analytical work directly: Islam and colleagues showed that the site-universality condition underlying the competitive Langmuir equation is violated by common lignocellulosic adsorbents, with the consequence that the model may reproduce capacities while failing to describe the equilibrium concentrations actually measured [11].

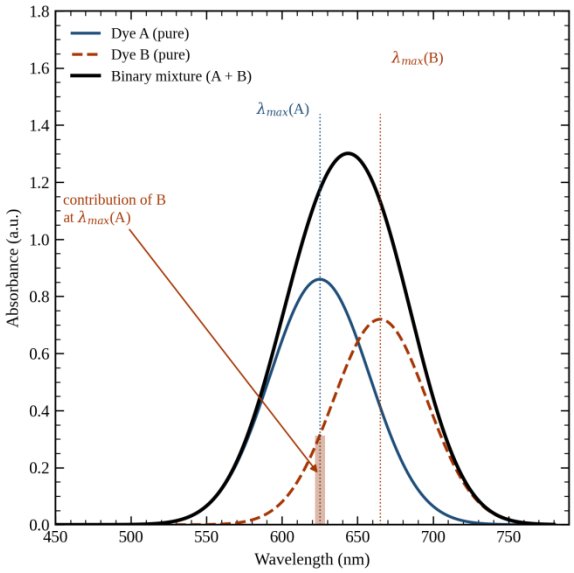

Figure 01: Origin of the quantification error in a binary dye system, shown with simulated Gaussian bands: pure-component visible spectra, the additive mixture spectrum, the wavelength positions commonly used for univariate measurement, and the shaded contribution of the second dye at the maximum of the first.

3. UNIVARIATE STRATEGIES: INEXPENSIVE, POPULAR AND EASY TO OVER-TRUST

3.1 Derivative spectrophotometry and the zero-crossing rule

Differentiating the absorption spectrum with respect to wavelength suppresses broad, slowly varying contributions and sharpens narrow ones. In the zero-crossing variant, analyte A is measured at a wavelength where the derivative signal of B is zero, so that the reading depends on A alone. The approach is old, well

understood, and its principal drawback is equally well known: each differentiation amplifies high-frequency noise, so the gain in resolution is paid for in signal-to-noise, and the derivative order and smoothing window must be optimised together rather than pushed as far as they will go [12].

Applications in adsorption are numerous. Gao and co-workers used first-order derivative spectrophotometry to follow the competitive biosorption of two anionic dyes on aerobic granules and were then able to fit multicomponent isotherms to genuine binary data [13]. Zolgharnein's group combined derivative calibration with a Box–Behnken design for brilliant green and crystal violet on surfactant-modified nano-alumina [14], and later applied the same logic to titan yellow with bromophenol blue on a polyaniline–silica composite [15] and to titan yellow with reactive blue 4 on a chitosan–hydroxyapatite material [16]. Asfaram and colleagues tracked malachite green and crystal violet individually despite what they described as significant interference in the visible region, and quantified the resulting drop in capacity when the two dyes were present together [17]. Aazza and co-workers applied first-derivative treatment specifically to overcome band overlap between o- and p-nitrophenol on alumina and modified alumina, obtaining kinetics and isotherms for both isomers [18]; the same isomer pair had been resolved much earlier by a hybrid of zero-crossing and peak-to-baseline measurement [19].

Ternary systems are considerably rarer, and they push the method harder. Ghaedi and co-workers needed fourth- and fifth-order derivatives to separate brilliant green from methylene blue on yeast biomass [20], a warning that the low-order case is not general. Third-order derivative signals with carefully chosen zero-crossing wavelengths were used for a crystal violet–brilliant green–methylene blue system on manganese dioxide-loaded activated carbon [21], second-order signals for a comparable triplet on copper sulfide-loaded carbon [22], and derivative measurement at 631, 592 and 377 nm resolved brilliant green, rhodamine B and methyl orange on cocoa-husk biochar [23]. A ternary anionic dye mixture on a calcined layered double hydroxide was treated in the same way and then interpreted with the help of density functional calculations [24].

3.2 Ratio spectra, double divisors and dual-wavelength measurement

Dividing the mixture spectrum by the spectrum of a pure standard, and then differentiating the resulting ratio, removes the divisor's contribution and is often more robust than direct differentiation. Extending the idea, the double-divisor ratio spectra derivative method uses the summed spectrum of two components as the divisor and thereby handles a three-component mixture without separation; the original demonstration was on a pharmaceutical triplet [25], but the algebra is indifferent to the analyte class. Dual-wavelength measurement, isosbestic-point strategies and normalised-spectra approaches form a related family whose rules for choosing wavelength pairs have been set out systematically for binary through quaternary mixtures [26]. A recent comparison applied derivative ratio zero-crossing, double-divisor ratio spectra and successive derivative subtraction to phenol, 2-aminophenol and 4-aminophenol in real water samples and scored each on greenness as well as accuracy, which is a useful precedent for environmental work [27].

3.3 The H-point standard addition method

The H-point standard addition method occupies an interesting middle position. Two standard-addition lines are constructed at a pair of wavelengths chosen so that the interferent's absorbance is equal at both; their intersection gives the analyte concentration free of the interferent's contribution, and also returns the interferent's own contribution [28]. Because the additions are made into the sample itself, the method compensates for proportional matrix effects, which is precisely what an adsorption supernatant needs. Its limitations are equally clear, and have been reviewed in detail: strict additivity and linear response are presumed, so any deviation from Beer's law biases the intersection point [29]. Despite its suitability, the method has been validated overwhelmingly on pharmaceutical formulations rather than on adsorption residuals, and this remains an obvious gap. Table 01 collects representative applications of these and the later strategies, together with the performance figures their authors reported.

Table 01: Representative chemometric strategies applied to the simultaneous quantification of co-existing pollutants in adsorption and related removal systems, with adsorbent or process, analyte set, method and reported performance.

Adsorbent or process	Co-existing pollutants (n)	Quantification strategy	Reported performance	Ref.
Bentonite	Basic Red 46 + Basic Yellow 28 (2)	First-derivative spectrophotometry	Single- and binary-solute isotherms; antagonistic competition	[7]
Inactive aerobic granules	Yellow 2G + Reactive Brilliant Red K-2G (2)	First-derivative, zero-crossing	Permitted extended Langmuir and Freundlich fitting of binary data	[13]
Saccharomyces cerevisiae biomass	Brilliant green + Methylene blue (2)	Fourth- and fifth-order derivative	Low-order derivatives insufficient for this dye pair	[20]
Ru nanoparticle-loaded activated carbon	Brilliant green + Methylene blue	High-order derivative	First-derivative treatment reported	[6]

	(2)		to fail	
Surfactant-modified nano-γ-Al_2O_3	Brilliant green + Crystal violet (2)	First derivative with Box–Behnken design	Linear 1–20 and 1–15 mg L^{-1}; LOD 0.3 and 0.5 mg L^{-1}	[14]
MnO_2 nanoparticle-loaded activated carbon	Crystal violet + Brilliant green + Methylene blue (3)	Third derivative, zero-crossing at 550, 440 and 710 nm	$r > 0.998$	[21]
CuS nanoparticle-loaded activated carbon	Ternary basic dye mixture (3)	Second-derivative spectrophotometry	Ternary removal optimised by response surface design	[22]
Cocoa pod husk biochar	Brilliant green + Rhodamine B + Methyl orange (3)	Derivative measurement at 631, 592 and 377 nm	Affinity order BG > RB > MO; NaCl-driven synergism	[23]
Polyaniline@SiO_2 nanocomposite	Titan yellow + Bromophenol blue (2)	Zero-crossing derivative	Binary uptake 129 and 109 against 141.5 and 129.6 mg g^{-1} alone	[15]
Chitosan@hydroxyapatite nanocomposite	Titan yellow + Reactive Blue 4 (2)	Zero-crossing derivative with central composite design	Method transferable across adsorbents and dye pairs	[16]
Al_2O_3 and $HDTMA^+/Al_2O_3$	o- and p-Nitrophenol (2)	First-derivative UV spectra	Binary capacities fall below the single-solute values	[18]
Calcined Mg(Al)O layered double hydroxide	Ternary anionic dye mixture (3)	Derivative spectrophotometry with DFT	Uptake order linked to computed adsorbate–surface interactions	[24]
Acid-treated okara	Acid Red 14 + Reactive Red 15 (2)	PLS regression	Single-solute q_{max} 217.4 and 243.9 mg g^{-1}; antagonistic binary uptake	[5]
Heated activated pine wood	Four food dyes (4)	PLS-1 and PCR	Recovery 96.2–103.6 %; error 2.3–6.9 %; LOD 0.11–0.29 mg L^{-1}; competition factors 0.64–0.77	[31]
Chemically activated pinewood biochar	Four colorants (4)	Kernel PLS	Recovery 96.7–103.4 %; error 1.4–9.4 %; combined retention 186.9 mg g^{-1}	[32]
Acid-activated kaolinitic clay	Brilliant blue + Brilliant black (2)	PLS	Accuracy 99.4–102.1 %; q_{max} 1644 and 1055 mg kg^{-1}; $\Delta H° \approx -21$ kJ mol^{-1}	[33]
Magnetic polymeric nanocomposite	Brilliant green + Malachite green (2)	PLS on original and first-derivative spectra	Test-set R^2 0.998 and 0.9996; RMSEP 0.12 and 0.19	[35]
Mandarin peel biosorbent	Four dyes with peel-derived colour	PLS-1 over 400–800 nm	$R^2 > 0.99$; RMSEP 0.013–0.93 mg L^{-1}	[8]
Cation-exchange fibres (solid-phase extraction)	Cu(II) + Ni(II) + Co(II) (3)	PLS after preconcentration	LOD 0.10, 0.13 and 0.15 µg L^{-1}; RSD < 5 %	[38]

AB-8 polymeric resin	Rutin + Quercetin (2)	PLS, stepwise regression and N-PLS	N-PLS predictions within 9 % of HPLC reference values	[60]
Granular activated carbon column	Eleven emerging contaminants with dissolved organic matter	EEM fluorescence with PARAFAC (five components)	Humic-like component predicted breakthrough across water matrices	[62]
Homogeneous Fenton treatment	Rhodamine B + Acid Red 14 (2)	MCR-ALS with a correlation constraint	Individual removal 81.6 and 80.2 %; optimised by response surface design	[66]
Polyamide microparticles	Bisphenol A followed in situ	Scattering correction with MCR-ALS	Adsorption kinetics obtained without filtration or sampling	[69]
Chitosan-based hybrid hydrogel	Acid Blue 9 + Allura Red (2)	Artificial neural network (5-10-10-10-2)	R = 0.9987; RMSE = 0.0119	[73]
Biogas digestate biochar	Methylene blue + Malachite green (2)	Principal component multivariate regression with IAST	IAST–Langmuir and IAST–Freundlich outperformed extended Langmuir	[82]
Seawater-spiked synthetic system	Crystal violet + Malachite green + Methylene blue (3)	PLS-1 and ANN with net analyte signal	R^2 0.997–0.999; error < 3 %; recovery 90–101 %	[36]

4. FIRST-ORDER MULTIVARIATE CALIBRATION

4.1 From principal component regression to partial least squares

First-order calibration uses the whole spectrum rather than a few wavelengths. Partial least squares, in its PLS-1 and PLS-2 forms, has become the default; the latent-variable model handles collinear and noisy spectra, and cross-validation provides a defensible rule for choosing the number of components [30]. In adsorption practice the results are remarkably consistent across systems. Al-Ghouti and co-workers resolved four spectrally overlapped food dyes on heated pine wood with recoveries between 96 and 104 per cent and extracted competition factors from the four-component isotherms [31]. The same group later used a kernel variant on an activated biochar [32] and conventional PLS on acid-activated kaolinitic clay, where the competition factors and the exothermic enthalpy of adsorption both followed from the resolved concentrations [33]. Zolgharnein and co-workers used PLS to overcome the alizarin red S–congo red overlap on cobalt hydroxide nanoparticles before optimising the removal conditions by response surface methodology [34], and Bagtash and Zolgharnein subsequently showed that building the PLS model on first-derivative rather than raw spectra improved prediction for a brilliant green–malachite green pair [35]. A ternary system of crystal violet, malachite green and methylene blue was handled equally well by PLS-1 and by a neural network, with the net analyte signal treatment allowing quantification in spiked seawater [36]. Binary isotherms of methylene blue and crystal violet on mandarin peels could only be extracted after a dedicated multivariate calibration step [37]. The approach is not restricted to dyes: solid-phase preconcentration followed by PLS deconvolution of overlapping charge-transfer bands gave sub-microgram per litre detection limits for copper, nickel and cobalt [38].

4.2 Pre-processing and variable selection

Two operations do most of the work in a good first-order model. Pre-processing removes what is not analyte information: scatter correction, baseline removal, Savitzky–Golay smoothing and derivatives, and mean centring, all of which have been systematically compared for their effect on the linearity of the signal–concentration relationship [39]. Orthogonal signal correction is a stronger variant that removes variance orthogonal to the concentration vector, and applying it before PLS roughly halved the prediction errors for the three nitrophenol isomers in water [40]. Variable selection then discards uninformative regions. Genetic algorithms tuned for spectroscopic data select contiguous, chemically interpretable regions rather than scattered single wavelengths [41]; the successive projections algorithm achieves a similar effect deterministically and reached comparable accuracy for a five-metal complex system using a fifth of the wavelengths [42]. Interval PLS and net-analyte-signal-guided selection have been used to quantify five overlapping colorants, in one case with only six variables [43], and moving-window implementations have been applied to disperse dyes in environmental samples [44].

4.3 Net analyte signal and analytical figures of merit

This is where the adsorption literature is weakest. The net analyte signal, that part of the signal orthogonal to the space spanned by all other constituents, is the basis for calculating sensitivity, selectivity, analytical sensitivity and detection limits in multivariate calibration. The framework was formalised in an IUPAC technical report [45] and later set out comprehensively for univariate through multiway models [46], along with practical guidance on how such results should be reported [47]. In practice, most multicomponent adsorption papers report only a correlation coefficient, a root-mean-square error of prediction and a recovery percentage. The elliptical joint confidence region for slope and intercept, which is the standard test of whether predicted and reference concentrations agree without proportional or constant bias, appears very seldom; among the studies surveyed here it was used in a soil-metal calibration with several variable-selection algorithms [48], but not in a competitive dye study. Since the competition factor is a ratio of capacities derived from these concentrations, an unstated calibration uncertainty becomes an unstated uncertainty in the mechanistic conclusion.

5. SECOND-ORDER AND MULTIWAY CHEMOMETRICS

5.1 The second-order advantage and why it matters here

The distinction between data orders is not a formality. Zero-order data, a single number per sample, require that no interferent be present. First-order data, a spectrum per sample, tolerate interferents provided they were included in the calibration set. Second-order data, a matrix per sample, allow accurate quantification even when an interferent was never calibrated at all, a property named the second-order advantage [49]. Figure 2 sets the hierarchy out visually and Table 2 gives the corresponding interference scenarios in more detail. Competitive adsorption is a textbook case for it, because the uncalibrated component is often exactly what cannot be anticipated: leached humic material, a partially degraded dye, or the coloured product of a side reaction at the surface. Multivariate curve resolution by alternating least squares, reviewed over fifty years of development, achieves this by decomposing a data matrix into concentration and spectral profiles under chemically meaningful constraints [50]. Extending the data set with several matrices, so-called multiset augmentation, can even confer the second-order advantage on data that are nominally first order [51].

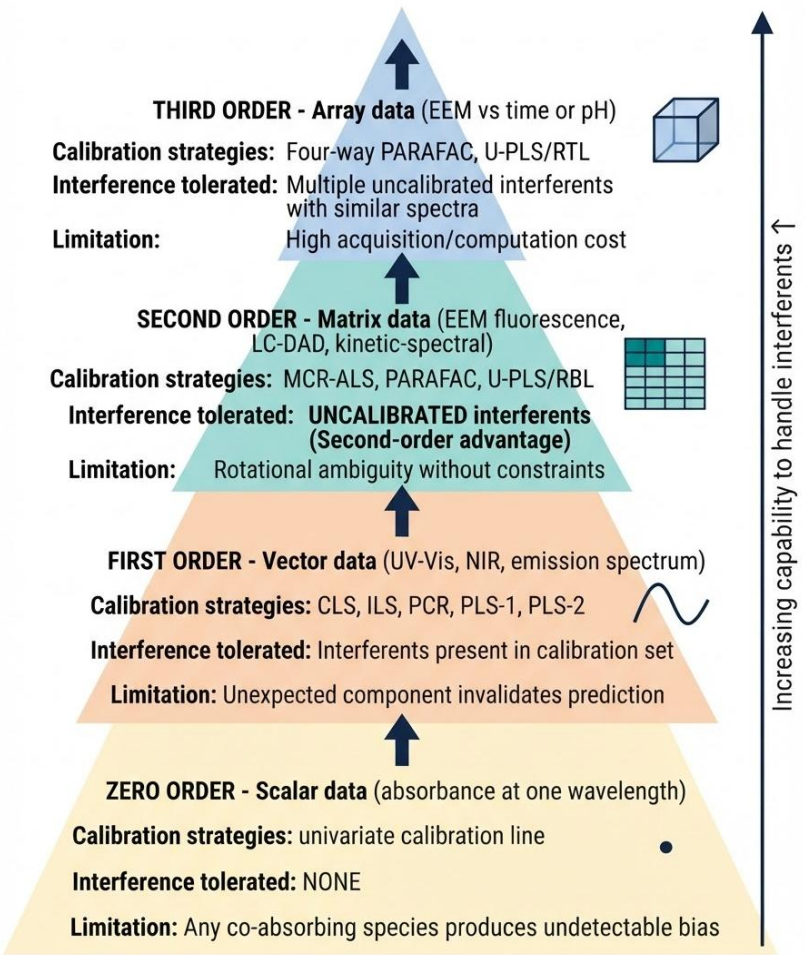

Figure 02: Hierarchy of data orders and the corresponding calibration strategies, with the interference scenario each level can and cannot handle.

Table 02: Comparison of zero-, first-, second- and third-order calibration with respect to the interference scenarios encountered in competitive adsorption experiments.

Data per sample	Typical measurement	Calibration approach	Interference tolerated	Principal limitation
Zero order (a scalar)	absorbance at one wavelength	univariate calibration line	none: the analyte must be the only absorbing species	any co-absorbing species produces a bias that cannot be detected [49]
First order (a vector)	full UV–Vis, NIR or emission scan	CLS, ILS, PCR, PLS-1 and PLS-2	interferents that were present in the calibration set	an unexpected component invalidates the prediction and shows only in the residuals [30, 49]
Second order (a matrix)	EEM fluorescence, LC-DAD, kinetic–spectral data	MCR-ALS, PARAFAC, U-PLS with residual bilinearisation	uncalibrated interferents, the second-order advantage	rotational ambiguity unless constraints and selectivity are adequate [50, 52, 54]
Third order (an array)	EEM recorded as a function of time or pH	four-way PARAFAC, U-PLS with residual trilinearisation	several uncalibrated interferents with nearly identical spectra	acquisition and computation cost; rarely available in adsorption laboratories [65]

5.2 Constraints, ambiguity and the honest limits of curve resolution

Bilinear decomposition is not unique on its own. Non-negativity, unimodality and closure narrow the family of admissible solutions but rarely reduce it to one, and the extent of the remaining rotational ambiguity can be computed by methods developed precisely for this purpose [52]. Additional constraints help: an area-correlation constraint applied to both calibration and unknown samples was shown to collapse the feasible region to a unique answer for severely overlapped, non-trilinear second-order data [53]. More recently it was demonstrated that the selectivity pattern of the pure spectra, and not the constraint set alone, determines whether curve resolution actually attains the second-order advantage in a given three-component system [54]. These are not academic subtleties. An adsorption paper reporting concentration profiles from curve resolution without stating the constraints applied, or without any assessment of ambiguity, is reporting one member of a family of solutions and calling it the answer.

5.3 Trilinear models and hyphenated data

Parallel factor analysis imposes trilinearity and gains essential uniqueness in return, which is why it dominates fluorescence work [55]. Where the trilinear assumption fails, as with chromatographic retention shifts, PARAFAC2 allows sample-specific profiles while preserving uniqueness [56], and a flexible, component-wise trilinearity constraint inside curve resolution has been shown to bridge the two situations for liquid chromatography with diode-array detection and related data [57]. For high-resolution mass spectrometry the regions-of-interest strategy compresses the data before resolution and has been applied to environmental extracts [58], with empirical quality metrics proposed more recently to make the parameter choices less arbitrary [59]. Multiway regression has also been taken directly into adsorption kinetics: comparing PLS, stepwise regression and multiway PLS on ultraviolet–visible spectra of a two-solute system on a polymeric resin, the multiway model predicted concentrations to within nine per cent of chromatographic reference values, which is a rare example of an independent instrumental check on a chemometric result in this field [60].

5.4 Fluorescence excitation–emission matrices and dissolved organic matter

Excitation–emission matrices are the most accessible source of second-order data, and the methodology for their PARAFAC analysis, including scatter handling and split-half validation, is well established [61]. The environmental relevance to competitive adsorption is direct. Sgroi and co-workers resolved five PARAFAC components from wastewater and surface water and found that the microbial humic-like component predicted the breakthrough of eleven co-existing emerging contaminants on granular activated carbon irrespective of the water matrix, effectively quantifying the competition exerted by natural organic matter for adsorption sites [62]. Tracking the same components through the unit operations of a full-scale drinking water plant showed which fractions are preferentially removed at each stage [63]. For pollutants themselves, excitation–emission data with unfolded PLS and residual bilinearisation quantified four pesticides at nanogram per millilitre levels in seawater despite humic interference [64], while a system of three fluoroquinolones with almost identical spectra required fourth-order data and the third-order advantage [65]. Degradation monitoring is a natural extension: curve resolution with a correlation constraint separated a binary dye mixture during Fenton treatment so that individual removal efficiencies could be optimised [66], parent quinolones were distinguished from their fluorescent transformation products in several water matrices [67], and the deethylation products of rhodamine B on a

titania film were resolved and validated against chromatography [68]. Most directly relevant of all, an inverse adding-doubling scattering correction combined with curve resolution allowed adsorption kinetics of bisphenol A on polyamide microparticles to be measured in situ, without filtration, from a single ultraviolet–visible measurement [69].

6. NEURAL NETWORKS AND MACHINE LEARNING

Nonlinearity enters multicomponent spectrophotometry through several doors: inner-filter effects at high absorbance, aggregation equilibria, and chemical interaction between the analytes. Where it is present, latent-variable regression is working against the data, and a nonlinear regressor becomes attractive. Principal component analysis coupled to a feed-forward network resolved a ternary mixture of food dyes with mean absolute errors below one per cent [70], and genetic-algorithm wavelength selection combined with a network outperformed both PLS-1 and genetic-algorithm PLS on a severely overlapped quaternary system [71]. A quite different application uses machine learning to identify as well as quantify: a self-attention architecture applied to surface-enhanced Raman spectra from combinations of probes quantified four coexisting metal ions in real effluents with errors below ten per cent [72].

Networks are also used on the adsorption side rather than the analytical side, and the two roles should not be confused. A multilayer perceptron reproduced single and competitive uptake of two dyes on a chitosan hybrid hydrogel with a correlation coefficient of 0.9987 [73], and ternary competitive adsorption on a fish-bone hydroxyapatite was modelled in the same way [74]. The most instructive comparison is older: for aqueous micropollutants on activated carbon cloth, neural networks reproduced the competitive equilibrium more accurately than ideal adsorbed solution theory, precisely because adsorbate–adsorbate interaction violates the ideal assumption [75]. Recent work extends this to predicting simultaneous removal of organics and metals using interpretable and generative approaches [76], and a systematic review of eighty-seven papers has codified the architectures and validation criteria that dye-adsorption modelling should meet [77]. The caution to be repeated is that a network with enough parameters will fit almost anything; without an external test set, and preferably an independent one, a high correlation coefficient means very little.

7. From concentrations to competition: propagating the analytical error

7.1 What the competitive models demand of the analyst

The extended or competitive Langmuir equation, whose origin lies in work from 1930 on species competing for a finite set of sites [78], requires single-solute constants and the equilibrium concentration of every component in the mixture. Ideal adsorbed solution theory predicts multicomponent equilibria from single-component isotherms through the equal-spreading-pressure criterion [79], and its fifty-year appraisal concluded that it performs well for near-ideal mixtures but fails systematically on energetically heterogeneous surfaces, with error in the single-component fit as the dominant propagated term [80]. Extended Freundlich, extended Sips and Langmuir–Freundlich variants often outperform extended Langmuir on real binary data; an arsenic–fluoride system on activated carbon was best described by the extended Langmuir–Freundlich form [81], and a binary methylene blue–malachite green system on digestate-derived biochar was fitted better by ideal adsorbed solution combinations than by extended Langmuir, but only after principal component regression had been used to resolve the overlapping spectra [82]. What each of these models demands of the analyst, and where each has been reported to break down, is summarised in Table 3.

Table 03: Competitive and multicomponent isotherm models, the concentration data each requires from the analytical step, and their documented limitations.

Model	Core assumption	Required from the analytical step	Documented limitation	Ref.
Competitive (extended) Langmuir	identical universal sites shared by all adsorbates; monolayer coverage	single-solute constants plus the equilibrium concentration of every component	the site-universality condition is violated by heterogeneous lignocellulosic surfaces, so capacities may be reproduced while equilibrium concentrations are not	[78, 11]
Extended Freundlich	empirical extension of the heterogeneous single-solute model	single-solute Freundlich constants and mixture concentrations	interaction coefficients are purely empirical and carry no thermodynamic meaning	[3]
Extended Sips and Langmuir–Freundlich	heterogeneous surface with a distribution of site energies	single-solute parameters and accurate mixture concentrations	more adjustable parameters than the data usually justify, giving strongly correlated estimates	[4, 81]
Ideal adsorbed solution theory	the adsorbed phase behaves as an ideal solution at equal spreading pressure	complete and well-fitted single-component isotherms over the whole range	fails on energetically heterogeneous adsorbents; error in the single-component fit is the dominant propagated term	[79, 80]
Neural net-	no explicit physical	a large, properly de-	no mechanistic interpretation, and	[75,

work or machine-learning surrogate	model is assumed	signed concentration matrix for training and independent testing	over-fitting whenever the test set is not truly independent	76]

7.2 The size of the effect

It is worth being concrete. The adsorbed amount is obtained by difference, q = V(C0 − Ce)/m, so a relative bias δ in the measured equilibrium concentration produces a relative error in capacity of δ(1 − R)/R, where R is the fractional removal. The algebra is unforgiving at low removal. A five per cent bias in Ce gives only about 1.3 per cent error in q at eighty per cent removal, but the same bias gives twenty per cent error at twenty per cent removal, and forty-five per cent at ten per cent removal (Figure 3). Since the competition factor is a ratio of capacities measured in mixture and in single solution, and the two biases need not have the same sign, the ratio can in the worst case inherit the sum of the two errors. Multiplied through a Langmuir fit over several points, this is enough to change which model is judged best and, in some cases, to turn a reported antagonistic interaction into an apparently non-interactive one. It also explains why the problem is most acute exactly where multicomponent work is most interesting, namely at the high initial concentrations and low removal efficiencies characteristic of competitive conditions. Very few papers propagate the analytical uncertainty into their isotherm parameters, and the omission deserves more attention than it receives.

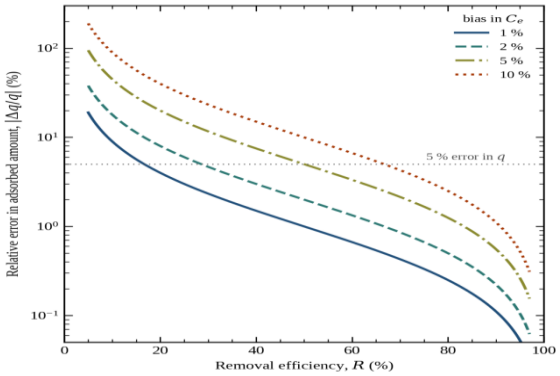

Figure 03: Propagation of a relative bias in the measured equilibrium concentration into the relative error of the adsorbed amount, as a function of removal efficiency, calculated from q = V(C0 − Ce)/m for bias levels of 1, 2, 5 and 10 per cent.

8. EXPERIMENTAL DESIGN AS PART OF THE ANALYTICAL STRATEGY

Design of experiments enters this field twice, and the two uses are often conflated. On the process side, Box–Behnken, central composite and related designs optimise pH, dose, contact time and initial concentrations for simultaneous removal, and this is now routine in the derivative-spectrophotometry papers cited above [14,16]. On the analytical side, the calibration set for a multivariate model is itself a designed experiment: concentrations of the analytes must be varied independently, over ranges that bracket the samples, with enough levels to support the number of latent variables. Multi-level factorial designs of this kind underpin the better-performing models [71], and where the design is weak the model tends to encode the correlation between analytes rather than their individual spectra. A calibration set built by diluting a single stock mixture is a common and serious error, since the analyte concentrations are then perfectly correlated and the model cannot distinguish them.

9. WHAT IS MISSING FROM CURRENT REPORTS

Before listing what is missing it is worth looking at what is actually used. Figure 4 shows how the application studies gathered for this review distribute across the method families and across binary, ternary and larger systems. Two things stand out. Derivative spectrophotometry and first-order multivariate calibration account for roughly two thirds of the corpus, and derivative work is overwhelmingly binary, whereas systems of four or more components are handled almost exclusively by multivariate or multiway methods. This is the expected pattern, and it is also a warning, since the binary case is the one in which a poor method is least likely to be caught.

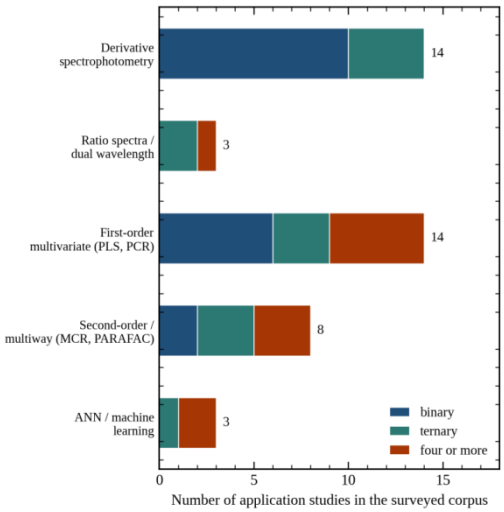

Figure 04: Distribution of quantification strategies across the application studies surveyed in this review, broken down by the number of co-existing components resolved. Studies applying more than one family are counted once, under the strategy on which their reported results rely.

Drawing the surveyed literature together, the recurring omissions are easy to list and easy to remedy. Additivity of the mixture spectrum is assumed rather than demonstrated. Calibration design is described in one line, if at all. Validation is reported as a correlation coefficient and a recovery, without root-mean-square error of prediction on an independent set, without the

elliptical joint confidence region, and without multivariate detection limits computed on the net analyte signal basis [46,47]. Where curve resolution is used, the constraints and the ambiguity assessment are usually absent [52,54]. Interference from the adsorbent itself is seldom quantified, although the tools exist [8,10]. And the analytical uncertainty is almost never carried forward into the isotherm parameters. None of these steps is expensive; together they would make competitive adsorption data comparable between laboratories in a way they currently are not. Table 4 sets them out as a checklist, and Figure 5 condenses the same reasoning into a decision path that can be followed before the first batch experiment is run rather than after the data have been collected.

Table 04: Proposed minimum reporting set for the analytical component of multicomponent adsorption studies.

Stage	Item to report	Why it matters
Preliminary checks	comparison of the mixture spectrum with the sum of the pure-component spectra at matched concentrations	establishes that additivity, on which every linear method depends, actually holds in the working range
Preliminary checks	spectrum of an adsorbent blank carried through the whole contact, filtration and dilution procedure	quantifies leached colour, turbidity and scattering before they are attributed to the pollutant
Calibration	design of the calibration set: levels per analyte, concentration ranges and evidence that analyte concentrations are not correlated	a set produced by diluting a single stock mixture cannot separate the analytes, whatever the algorithm
Calibration	pre-processing applied and, for latent-variable models, the number of components together with the selection criterion	makes the model reproducible and guards against over-fitting
Validation	root-mean-square error of prediction on an independent test set, not cross-validation alone	cross-validation is optimistic, particularly for the small calibration sets typical of this field
Validation	elliptical joint confidence region for the slope and intercept of predicted against reference concentrations	the standard test for proportional and constant bias, and almost never reported
Validation	multivariate limits of detection and quantification computed on a net analyte signal basis	univariate detection limits are not transferable to multivariate models
Curve resolution	the constraints applied and an assessment of the remaining rotational ambiguity	without them one member of a family of solutions is being reported as the answer
Adsorption modelling	propagation of the analytical uncertainty into capacities, competition factors and isotherm constants	the mechanistic conclusion is only as reliable as the concentrations that support it

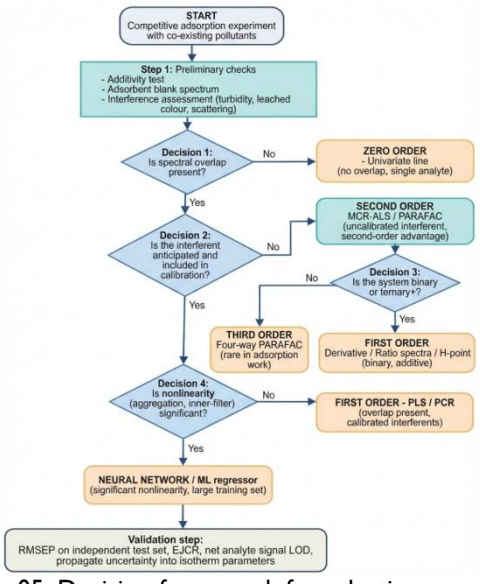

Figure 05: Decision framework for selecting a quantification strategy in competitive adsorption experiments, from the preliminary additivity and interference checks through to the choice of calibration order.

10. OUTLOOK

Three directions seem likely to matter. First, in situ measurement. The demonstration that adsorption kinetics can be followed without filtration by combining a scattering correction with curve resolution [69] points to a class of experiments in which the sampling step, itself a source of error and of adsorbate loss, disappears; extending that from one adsorbate to a competing pair is a natural next study. Second, portable and low-cost instrumentation. Smartphone-based colorimetry and inexpensive spectrometers generate data of adequate quality for chemometric treatment, and would allow multicomponent removal to be monitored where it actually happens rather than in a laboratory some distance away. Third, standardisation. The analytical chemistry community has produced clear guidance on how multivariate calibration should be validated and reported [45,47]; the adsorption community has largely not adopted it. A short, agreed checklist, endorsed by the journals that publish most of this work, would probably do more for data quality than any new algorithm. It would also make the growing body of machine-learning work more useful, since those models are only as good as the concentrations they are trained on [77,76].

11. CONCLUSION

The analytical step in competitive adsorption research has been treated as a routine preliminary for far too long, when in fact it determines whether the thermodynamic and mechanistic conclusions mean anything. The evidence assembled here is fairly unambiguous. Single-wavelength photometry is unsafe in any multicomponent system, and the primary literature contains explicit reports of its failure. Derivative and ratio-spectra methods are inexpensive and effective for binary systems, provided that additivity holds and suitable zero-crossing wavelengths exist, but they degrade quickly with increasing derivative order and with the number of components. First-order multivariate calibration is the practical workhorse and handles calibrated interferents well. Only second-order and multiway methods cope reliably with the uncalibrated interferences that adsorption experiments generate, and their trustworthiness depends on constraints and ambiguity assessment that are rarely reported. Neural networks are valuable where nonlinearity is genuine, and misleading where validation is thin. Above all, the uncertainty of the quantification step should be estimated, stated and propagated into the competition factors and isotherm constants that the study is really about. Doing so consistently would cost very little and would substantially raise the credibility of a large and growing literature.

12. FUNDING INFORMATION

This research received no specific grant from any funding agency in the public, commercial, or not-for-profit sectors.

13. ETHICS STATEMENT

This study did not involve human or animal subjects and, therefore, did not require ethical approval.

14. STATEMENT OF CONFLICT OF INTERESTS

The authors declare no conflicts of interest related to this study.

16. REFERENCES

1. Bayuo J, Rwiza MJ, Sillanpää M, Mtei KM. Removal of heavy metals from binary and multicomponent adsorption systems using various adsorbents – a systematic review. RSC Adv. 2023; 13(19): 13052-13093. https://doi.org/10.1039/D3RA01660A
2. Akhtar N, Aslam Z, Shawabkeh RA, Baig N, Aslam U, Ihsanullah, et al. Decolorization of multicomponent dye-laden wastewater by modified waste fly ash: a parametric analysis for an anionic and cationic combination of dyes. Environ Sci Pollut Res. 2023; 30(31): 77165-77180. https://doi.org/10.1007/s11356-023-27671-1
3. Amrutha, Jeppu G, Girish CR, Prabhu B, Mayer K. Multi-component adsorption isotherms: review and modeling studies. Environ Process. 2023; 10(2): 38. https://doi.org/10.1007/s40710-023-00631-0
4. Sharma K, Dalai AK, Vyas RK. Removal of synthetic dyes from multicomponent industrial wastewaters. Rev Chem Eng. 2018; 34(1): 107-134. https://doi.org/10.1515/revce-2016-0042
5. Gao JF, Wang JH, Yang C, Wang SY, Peng YZ. Binary biosorption of Acid Red 14 and Reactive Red 15 onto acid treated okara: simultaneous spectrophotometric determination of two dyes using partial least squares regression. Chem Eng J. 2011; 171(3): 967-975. https://doi.org/10.1016/j.cej.2011.04.047
6. Hajati S, Ghaedi M, Barazesh B, Karimi F, Sahraei R, Daneshfar A, et al. Application of high order derivative spectrophotometry to resolve the spectra overlap between BG and MB for the simultaneous determination of them: ruthenium nanoparticle loaded activated carbon as adsorbent. J Ind Eng Chem. 2014; 20(4): 2421-2427. https://doi.org/10.1016/j.jiec.2013.10.022
7. Turabik M. Adsorption of basic dyes from single and binary component systems onto bentonite: simultaneous analysis of Basic Red 46 and Basic Yellow 28 by first order derivative spectrophotometric analysis method. J Hazard Mater. 2008; 158(1): 52-64. https://doi.org/10.1016/j.jhazmat.2008.01.033
8. Besegatto SV, Martins ML, Lopes TJ, da Silva A. Multivariated calibration as a tool for resolution of color from mandarin peel and dyes in aqueous solution for bioadsorption studies. J Environ Chem Eng. 2021; 9(1): 104605. https://doi.org/10.1016/j.jece.2020.104605

9. Xia H, Yang Y, Zhang W, Yang Z, Dai Z. Spectrophotometric determination of p-nitrophenol under ENP interference. J Anal Methods Chem. 2021; 2021: 6682722. https://doi.org/10.1155/2021/6682722
10. Antony A, Mitra J. Refractive index-assisted UV/Vis spectrophotometry to overcome spectral interference by impurities. Anal Chim Acta. 2021; 1149: 238186. https://doi.org/10.1016/j.aca.2020.12.061
11. Islam MA, Choudhury JT, Hossain F, Uddin MT. Competitive Langmuir model for dye mixture adsorption: disagreement between theoretical ground and application condition. Langmuir. 2025; 41(1): 216-230. https://doi.org/10.1021/acs.langmuir.4c03340
12. Karpińska J. Derivative spectrophotometry – recent applications and directions of developments. Talanta. 2004; 64(4): 801-822. https://doi.org/10.1016/j.talanta.2004.03.060
13. Gao JF, Zhang Q, Su K, Wang JH. Competitive biosorption of Yellow 2G and Reactive Brilliant Red K-2G onto inactive aerobic granules: simultaneous determination of two dyes by first-order derivative spectrophotometry and isotherm studies. Bioresour Technol. 2010; 101(15): 5793-5801. https://doi.org/10.1016/j.biortech.2010.02.091
14. Zolgharnein J, Bagtash M, Shariatmanesh T. Simultaneous removal of binary mixture of Brilliant Green and Crystal Violet using derivative spectrophotometric determination, multivariate optimization and adsorption characterization of dyes on surfactant modified nano-γ-alumina. Spectrochim Acta A Mol Biomol Spectrosc. 2015; 137: 1016-1028. https://doi.org/10.1016/j.saa.2014.08.115
15. Rastgordani M, Zolgharnein J, Mahdavi V. Derivative spectrophotometry and multivariate optimization for simultaneous removal of Titan yellow and Bromophenol blue dyes using polyaniline@SiO2 nanocomposite. Microchem J. 2020; 155: 104717. https://doi.org/10.1016/j.microc.2020.104717
16. Rastgordani M, Zolgharnein J. Simultaneous determination and optimization of Titan yellow and Reactive Blue 4 dyes removal using chitosan@hydroxyapatite nanocomposites. J Polym Environ. 2021; 29(6): 1789-1807. https://doi.org/10.1007/s10924-020-01982-7
17. Asfaram A, Ghaedi M, Ghezelbash GR, Pepe F. Application of experimental design and derivative spectrophotometry methods in optimization and analysis of biosorption of binary mixtures of basic dyes from aqueous solutions. Ecotoxicol Environ Saf. 2017; 139: 219-227. https://doi.org/10.1016/j.ecoenv.2017.01.043
18. Aazza M, Mounir C, Ahlafi H, Bouymajane A, Cacciola F. Performance of first derivative UV/Visible spectra for kinetic and isothermal study of simultaneous adsorption of o-nitrophenol and p-nitrophenol onto Al2O3 and HDTMA+/Al2O3 composite. J Mol Liq. 2023; 383: 122139. https://doi.org/10.1016/j.molliq.2023.122139
19. Toral MI, Richter P, Cavieres M, González W. Simultaneous determination of o- and p-nitrophenol by first derivative spectrophotometry. Environ Monit Assess. 1999; 54(2): 191-203. https://doi.org/10.1023/A:1005977421221
20. Ghaedi M, Hajati S, Barazesh B, Karimi F, Ghezelbash G. Saccharomyces cerevisiae for the biosorption of basic dyes from binary component systems and the high order derivative spectrophotometric method for simultaneous analysis of Brilliant green and Methylene blue. J Ind Eng Chem. 2013; 19(1): 227-233. https://doi.org/10.1016/j.jiec.2012.08.006
21. Asfaram A, Ghaedi M, Hajati S, Goudarzi A. Ternary dye adsorption onto MnO2 nanoparticle-loaded activated carbon: derivative spectrophotometry and modeling. RSC Adv. 2015; 5(88): 72300-72320. https://doi.org/10.1039/C5RA10815B
22. Bagheri AR, Ghaedi M, Asfaram A, Hajati S, Ghaedi AM, Bazrafshan A, et al. Modeling and optimization of simultaneous removal of ternary dyes onto copper sulfide nanoparticles loaded on activated carbon using second-derivative spectrophotometry. J Taiwan Inst Chem Eng. 2016; 65: 212-224. https://doi.org/10.1016/j.jtice.2016.05.004
23. Córdova BM, Santa Cruz JP, Ocampo M TV, Huamani-Palomino RG, Baena-Moncada AM. Simultaneous adsorption of a ternary mixture of brilliant green, rhodamine B and methyl orange as artificial wastewater onto biochar from cocoa pod husk waste. Quantification of dyes using the derivative spectrophotometry method. New J Chem. 2020; 44(19): 8303-8316. https://doi.org/10.1039/D0NJ00916D
24. Jabkhiro H, El Hassani K, Chems M, Anouar A. Simultaneous removal of anionic dyes onto Mg(Al)O mixed metal oxides from ternary aqueous mixture: derivative spectrophotometry and density functional theory study. Colloid Interface Sci Commun. 2021; 45: 100549. https://doi.org/10.1016/j.colcom.2021.100549
25. Dinç E. The spectrophotometric multicomponent analysis of a ternary mixture of ascorbic acid, acetylsalicylic acid and paracetamol by the double divisor-ratio spectra derivative and ratio spectra-zero crossing methods. Talanta. 1999; 48(5): 1145-1157. https://doi.org/10.1016/S0039-9140(98)00337-3
26. Mohamed EH, Lotfy HM, Hegazy MA, Mowaka S. Different applications of isosbestic points, normalized spectra and dual wavelength as powerful tools for resolution of multicomponent mixtures with severely overlapping spectra. Chem Cent J. 2017; 11(1): 43. https://doi.org/10.1186/s13065-017-0270-8
27. Mustafa MS, Mohammad NN, Radha FH, Kayani KF, Ghareeb HO, Mohammed SJ. Eco-friendly spectrophotometric methods for concurrent analysis of phenol, 2-aminophenol, and 4-aminophenol in ternary mixtures and water samples: assessment of environmental sustainability.

RSC Adv. 2024; 14(23): 16045-16055. https://doi.org/10.1039/D4RA01094A
28. Bosch Reig F, Campins Falcó P. H-point standard additions method. Part 1. Fundamentals and application to analytical spectroscopy. Analyst. 1988; 113(7): 1011-1016. https://doi.org/10.1039/AN9881301011
29. Al-Sabha TN, Bunaciu AA, Aboul-Enein HY. H-point standard addition method (HPSAM) in simultaneous spectrophotometric determination of binary mixtures: an overview. Appl Spectrosc Rev. 2011; 46(8): 607-623. https://doi.org/10.1080/05704928.2011.570836
30. Wold S, Sjöström M, Eriksson L. PLS-regression: a basic tool of chemometrics. ChemomIntell Lab Syst. 2001; 58(2): 109-130. https://doi.org/10.1016/S0169-7439(01)00155-1
31. Al-Ghouti MA, Issa AA, Al-Saqarat BS, Al-Reyahi AY, Al-Degs YS. Multivariate analysis of competitive adsorption of food dyes by activated pine wood. Desalin Water Treat. 2016; 57(57): 27651-27662. https://doi.org/10.1080/19443994.2016.1174742
32. Issa AA, Al-Degs YS, El-Sheikh AH, Al-Reyahi AY, Al Bakain RZ, Abdelghani JI, et al. Application of partial least squares–kernel calibration in competitive adsorption studies using an effective chemically activated biochar. CLEAN – Soil Air Water. 2017; 45(5): 1600333. https://doi.org/10.1002/clen.201600333
33. Issa AA, Abdel-Halim HM, Al-Degs YS, Al-Masri HA. Application of multivariate calibration for studying competitive adsorption of two problematic colorants on acid-activated-kaolinitic clay. Res Chem Intermed. 2017; 43(1): 523-544. https://doi.org/10.1007/s11164-016-2638-0
34. Zolgharnein J, Bagtash M, Asanjarani N. Chemometrics approach for optimization of simultaneous adsorption of Alizarin red S and Congo red by cobalt hydroxide nanoparticles. J Chemom. 2017; 31(2): e2886. https://doi.org/10.1002/cem.2886
35. Bagtash M, Zolgharnein J. Removal of brilliant green and malachite green from aqueous solution by a viable magnetic polymeric nanocomposite: simultaneous spectrophotometric determination of 2 dyes by PLS using original and first derivative spectra. J Chemom. 2018; 32(3): e3014. https://doi.org/10.1002/cem.3014
36. Hassaninejad-Darzi SK, Torkamanzadeh M. Simultaneous UV-Vis spectrophotometric quantification of ternary basic dye mixtures by partial least squares and artificial neural networks. Water Sci Technol. 2016; 74(10): 2497-2504. https://doi.org/10.2166/wst.2016.440
37. Lima JP, Besegatto SV, Villanueva-Mejía F, García-Hernández E, Bonilla-Petriciolet A, Lopes TJ. Binary adsorption isotherms of methylene blue and crystal violet on mandarin peels: prediction via detailed multivariate calibration and density functional theory (DFT) calculations. Environ Sci Pollut Res. 2023; 30(39): 92436-92450. https://doi.org/10.1007/s11356-023-28873-3
38. Guo Y, Zhao H, Han Y, Liu X, Guan S, Zhang Q, et al. Simultaneous spectrophotometric determination of trace copper, nickel, and cobalt ions in water samples using solid phase extraction coupled with partial least squares approaches. Spectrochim Acta A Mol Biomol Spectrosc. 2017; 173: 532-536. https://doi.org/10.1016/j.saa.2016.10.003
39. Rinnan Å, van den Berg F, Engelsen SB. Review of the most common pre-processing techniques for near-infrared spectra. TrAC Trends Anal Chem. 2009; 28(10): 1201-1222. https://doi.org/10.1016/j.trac.2009.07.007
40. Niazi A, Yazdanipour A. Spectrophotometric simultaneous determination of nitrophenol isomers by orthogonal signal correction and partial least squares. J Hazard Mater. 2007; 146(1-2): 421-427. https://doi.org/10.1016/j.jhazmat.2007.03.063
41. Leardi R. Application of genetic algorithm-PLS for feature selection in spectral data sets. J Chemom. 2000; 14(5-6): 643-655. https://doi.org/10.1002/1099-128X(200009/12)14:5/6<643::AID-CEM621>3.0.CO;2-E
42. Araújo MCU, Saldanha TCB, Galvão RKH, Yoneyama T, Chame HC, Visani V. The successive projections algorithm for variable selection in spectroscopic multicomponent analysis. ChemomIntell Lab Syst. 2001; 57(2): 65-73. https://doi.org/10.1016/S0169-7439(01)00119-8
43. Al-Degs YS, El-Sheikh AH, Saleh AI, Al-Reyahi AY. Interval wavelength selection and simultaneous quantification of spectrally overlapping food colorants by multivariate calibration. J Food Meas Charact. 2021; 15(3): 2562-2575. https://doi.org/10.1007/s11694-021-00848-3
44. Şahin S, Sarıburun E, Demir C. Net analyte signal-based simultaneous determination of dyes in environmental samples using moving window partial least squares regression with UV-vis spectroscopy. Anal Methods. 2009; 1(3): 208-214. https://doi.org/10.1039/b9ay00009g
45. Olivieri AC, Faber NM, Ferré J, Boqué R, Kalivas JH, Mark H. Uncertainty estimation and figures of merit for multivariate calibration (IUPAC Technical Report). Pure Appl Chem. 2006; 78(3): 633-661. https://doi.org/10.1351/pac200678030633
46. Olivieri AC. Analytical figures of merit: from univariate to multiway calibration. Chem Rev. 2014; 114(10): 5358-5378. https://doi.org/10.1021/cr400455s
47. Olivieri AC. Practical guidelines for reporting results in single- and multi-component analytical calibration: a tutorial. Anal Chim Acta. 2015; 868: 10-22. https://doi.org/10.1016/j.aca.2015.01.017
48. Abrantes G, Almeida V, Maia AJ, Nascimento R, Nascimento C, Silva Y, et al. Comparison between variable-selection algorithms in PLS regression with near-infrared spectroscopy to predict se-

lected metals in soil. Molecules. 2023; 28(19): 6959. https://doi.org/10.3390/molecules28196959
49. Olivieri AC. Analytical advantages of multivariate data processing. One, two, three, infinity? Anal Chem. 2008; 80(15): 5713-5720. https://doi.org/10.1021/ac800692c
50. de Juan A, Tauler R. Multivariate curve resolution: 50 years addressing the mixture analysis problem – a review. Anal Chim Acta. 2021; 1145: 59-78. https://doi.org/10.1016/j.aca.2020.10.051
51. Mazivila SJ, Santos JLM. A review on multivariate curve resolution applied to spectroscopic and chromatographic data acquired during the real-time monitoring of evolving multi-component processes: from process analytical chemistry (PAC) to process analytical technology (PAT). TrAC Trends Anal Chem. 2022; 157: 116698. https://doi.org/10.1016/j.trac.2022.116698
52. Golshan A, Abdollahi H, Beyramysoltan S, Maeder M, Neymeyr K, Rajkó R, et al. A review of recent methods for the determination of ranges of feasible solutions resulting from soft modelling analyses of multivariate data. Anal Chim Acta. 2016; 911: 1-13. https://doi.org/10.1016/j.aca.2016.01.011
53. Ghaffari M, Olivieri AC, Abdollahi H. Strategy to obtain accurate analytical solutions in second-order multivariate calibration with curve resolution methods. Anal Chem. 2018; 90(16): 9725-9733. https://doi.org/10.1021/acs.analchem.8b00336
54. Chiappini FA, Pinto L, Alcaraz MR, Omidikia N, Goicoechea HC, Olivieri AC. Multivariate curve resolution-alternating least-squares and second-order advantage in first-order calibration. A systematic characterisation for three-component analytical systems. Anal Chim Acta. 2024; 1328: 343159. https://doi.org/10.1016/j.aca.2024.343159
55. Bro R. PARAFAC. Tutorial and applications. ChemomIntell Lab Syst. 1997; 38(2): 149-171. https://doi.org/10.1016/S0169-7439(97)00032-4
56. Bro R, Andersson CA, Kiers HAL. PARAFAC2 – Part II. Modeling chromatographic data with retention time shifts. J Chemom. 1999; 13(3-4): 295-309. https://doi.org/10.1002/(SICI)1099-128X(199905/08)13:3/4<295::AID-CEM547>3.0.CO;2-Y
57. Zhang X, Tauler R. Flexible implementation of the trilinearity constraint in multivariate curve resolution alternating least squares (MCR-ALS) of chromatographic and other type of data. Molecules. 2022; 27(7): 2338. https://doi.org/10.3390/molecules27072338
58. Pérez-López C, Oró-Nolla B, Lacorte S, Tauler R. Regions of interest multivariate curve resolution liquid chromatography with data-independent acquisition tandem mass spectrometry. Anal Chem. 2023; 95(19): 7519-7527. https://doi.org/10.1021/acs.analchem.2c05704
59. Benedetti B, Pérez-López C, MacKeown H, Magi E, Tauler R. Improving regions of interest multivariate curve resolution: development of an empirical metric system through the study of passive sampling extracts of wastewater in Antarctica. Anal Chem. 2025; 97(31): 13110-13119. https://doi.org/10.1021/acs.analchem.5c00777
60. Yang X, Muhammad T, Bakri M, Muhammad I, Yang J, Zhai H, et al. Simple and fast spectrophotometric method based on chemometrics for the measurement of multicomponent adsorption kinetics. J Chemom. 2020; 34(8): e3249. https://doi.org/10.1002/cem.3249
61. Murphy KR, Stedmon CA, Graeber D, Bro R. Fluorescence spectroscopy and multi-way techniques. PARAFAC. Anal Methods. 2013; 5(23): 6557-6566. https://doi.org/10.1039/c3ay41160e
62. Sgroi M, Anumol T, Roccaro P, Vagliasindi FGA, Snyder SA. Modeling emerging contaminants breakthrough in packed bed adsorption columns by UV absorbance and fluorescing components of dissolved organic matter. Water Res. 2018; 145: 667-677. https://doi.org/10.1016/j.watres.2018.09.018
63. Sciscenko I, Binetti R, Escudero-Oñate C, Oller I, Arques A. Dissolved organic matter behaviour by conventional treatments of a drinking water plant: controlling its changes with EEM-PARAFAC. Appl Sci. 2024; 14(6): 2462. https://doi.org/10.3390/app14062462
64. Yuan YY, Wang ST, Liu SY, Cheng Q, Wang ZF, Kong DM. Green approach for simultaneous determination of multi-pesticide residue in environmental water samples using excitation-emission matrix fluorescence and multivariate calibration. Spectrochim Acta A Mol Biomol Spectrosc. 2020; 228: 117801. https://doi.org/10.1016/j.saa.2019.117801
65. Osorio A, Toledo-Neira C, Bravo MA. Critical evaluation of third-order advantage with highly overlapped spectral signals. Determination of fluoroquinolones in fish-farming waters by fluorescence spectroscopy coupled to multivariate calibration. Talanta. 2019; 204: 438-445. https://doi.org/10.1016/j.talanta.2019.06.048
66. Aliasgharlou N, Bahram M, Zolfaghari P, Mohseni N. Modeling and optimization of simultaneous degradation of rhodamine B and acid red 14 binary solution by homogeneous Fenton reaction: a chemometrics approach. Turk J Chem. 2020; 44(4): 987-1001. https://doi.org/10.3906/kim-2002-59
67. Sciscenko I, Mora M, Micó P, Escudero-Oñate C, Oller I, Arques A. EEM-PARAFAC as a convenient methodology to study fluorescent emerging pollutants degradation: (fluoro)quinolones oxidation in different water matrices. Sci Total Environ. 2022; 852: 158338. https://doi.org/10.1016/j.scitotenv.2022.158338
68. Morales JMN, Alcaraz MR, Loto A, Parellada EA, Tulli F, Morán Vieyra FE, et al. Chemometric modeling of spectroscopic data for characterizing the

visible-light-driven photocatalytic N-dealkylation of rhodamine B on a TiO2 film. PhotochemPhotobiol. 2025; 101(4): 1000-1012. https://doi.org/10.1111/php.14043
69. Yang XD, Gong B, Chen W, Chen JJ, Qian C, Lu R, et al. In situ quantitative monitoring of adsorption from aqueous phase by UV–vis spectroscopy: implication for understanding of heterogeneous processes. Adv Sci. 2024; 11(35): 2402732. https://doi.org/10.1002/advs.202402732
70. Estrada-Moreno JC, Rendon-Lara E, Jiménez-Núñez ML. Combination of artificial neural networks and principal component analysis for the simultaneous quantification of dyes in multicomponent aqueous mixtures. Appl Sci. 2024; 14(2): 809. https://doi.org/10.3390/app1402809
71. Kelani KM, Fekry RA, Fayez YM, Hassan SA. Advanced chemometric methods for simultaneous quantitation of caffeine, codeine, paracetamol, and p-aminophenol in their quaternary mixture. Sci Rep. 2024; 14(1): 2085. https://doi.org/10.1038/s41598-024-52450-4
72. Li F, Chao S, Wang X, Hu Z, Wang D, Tang C, et al. AI-enhanced SERS with probe combinations for concurrent identification and quantification of coexisting metal ions in water. Environ Sci Technol. 2025; 59(35): 17322-17333. https://doi.org/10.1021/acs.est.5c07025
73. Pauletto PS, Gonçalves JO, Pinto LAA, Dotto GL, Salau NPG. Single and competitive dye adsorption onto chitosan-based hybrid hydrogels using artificial neural network modeling. J Colloid Interface Sci. 2020; 560: 722-729. https://doi.org/10.1016/j.jcis.2019.10.106
74. Duarte EDV, Ribeiro NFP, Silva MGC, Vieira MGA, Carvalho SML. Pirarucu hydroxyapatite applied to ternary competitive adsorption of synthetic basic dyes as contaminants of emerging concern: kinetic, equilibrium, and ANN studies. Environ Sci Pollut Res. 2024; 31(18): 26942-26960. https://doi.org/10.1007/s11356-024-32968-w
75. Monneyron P, Faur-Brasquet C, Sakoda A, Suzuki M, Le Cloirec P. Competitive adsorption of organic micropollutants in the aqueous phase onto activated carbon cloth: comparison of the IAS model and neural networks in modeling data. Langmuir. 2002; 18(13): 5163-5169. https://doi.org/10.1021/la020023m
76. Zhai M, Wu Z, Fu B, Sun J, Sleiman M, Meunier FC, et al. Interpretable-generative machine learning approaches for predicting simultaneous removal of organic pollutants and heavy metals from water by adsorbent materials. J Clean Prod. 2025; 532: 146980. https://doi.org/10.1016/j.jclepro.2025.146980
77. da Costa MFP, Araújo RS, Silva AR, Pereira L, Silva GMM. Predictive artificial neural networks as applied tools in the remediation of dyes by adsorption – a review. Appl Sci. 2025; 15(5): 2310. https://doi.org/10.3390/app15052310
78. Butler JAV, Ockrent C. Studies in electrocapillarity. III. J Phys Chem. 1930; 34(12): 2841-2859. https://doi.org/10.1021/j150318a015
79. Myers AL, Prausnitz JM. Thermodynamics of mixed-gas adsorption. AIChE J. 1965; 11(1): 121-127. https://doi.org/10.1002/aic.690110125
80. Walton KS, Sholl DS. Predicting multicomponent adsorption: 50 years of the ideal adsorbed solution theory. AIChE J. 2015; 61(9): 2757-2762. https://doi.org/10.1002/aic.14878
81. Acharya A, Jeppu G, Girish CR, Prabhu B, Murty VR, Martis AS, et al. Adsorption of arsenic and fluoride: modeling of single and competitive adsorption systems. Heliyon. 2024; 10(12): e31967. https://doi.org/10.1016/j.heliyon.2024.e31967
82. Duong VH, Phuong PX, Thuan PTD, Taisheva A, Dung DV, Phung LD, et al. A novel treatment of biogas digestate waste for biochar production and its adsorption of methylene blue and malachite green in a binary system. Biofuels BioprodBiorefin. 2025; 19(8): 1728-1745. https://doi.org/10.1002/bbb.2772